Supplementary Information

Here, we present supplementary information to the paper called *"Electrical Conductivity Characteristics of a Locked Fault: Investigation of Ganos Segment on the North Anatolian Fault by Three-dimensional Magnetotellurics"*. It consists of additional data and figures that was important during interpretation, but was not necessary for the presentation.

Validity of ModEM results - Wide-band MT Fitting Curves

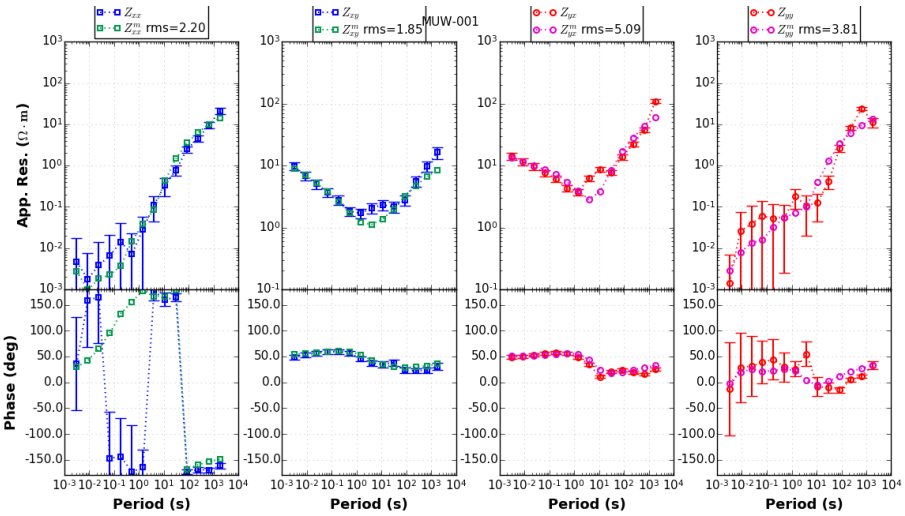

Figure 1: Model fitting curve for station MUW-001

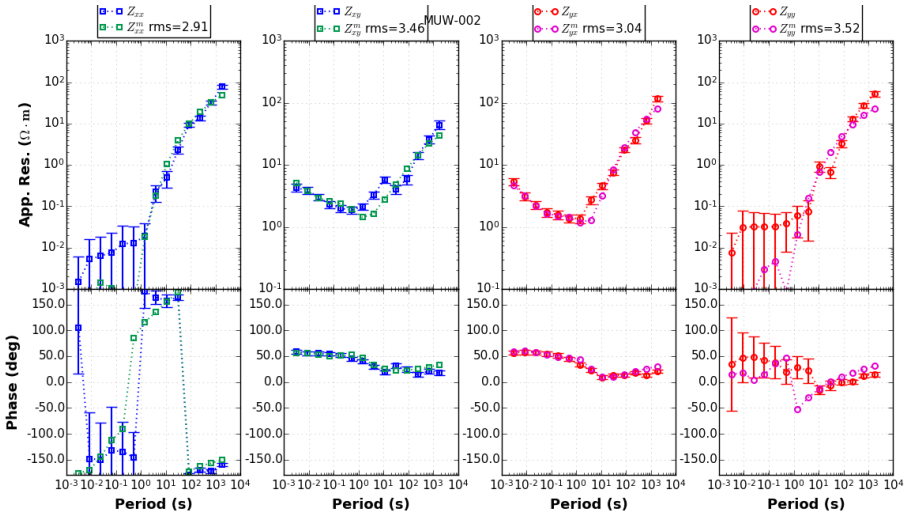

Figure 2: Model fitting curve for station MUW-002

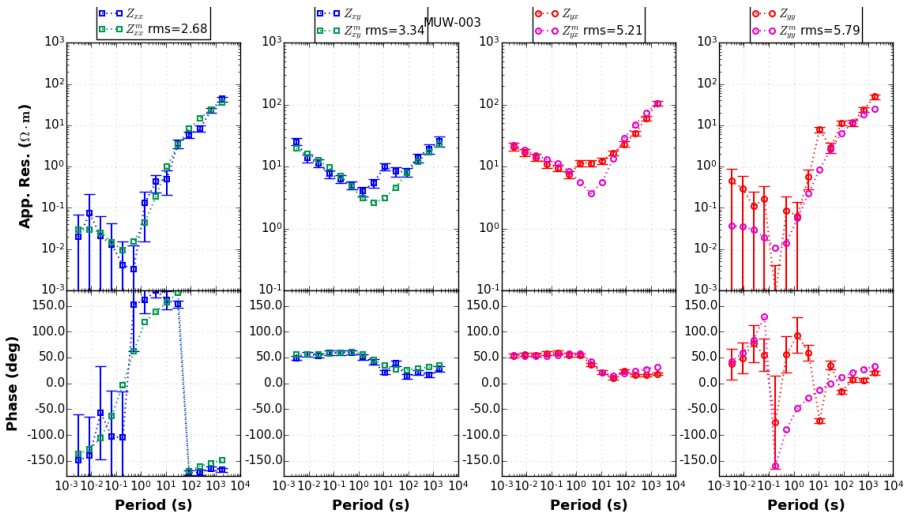

Figure 3: Model fitting curve for station MUW-003

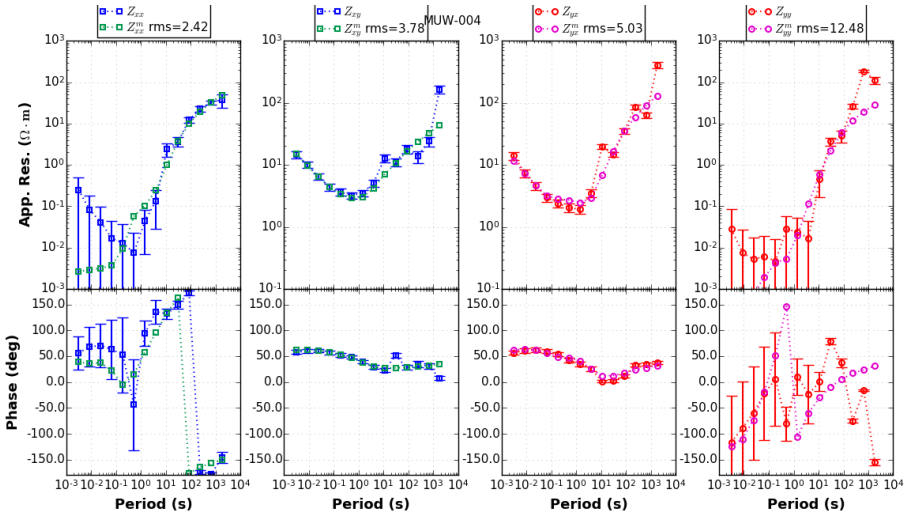

Figure 4: Model fitting curve for station MUW-004

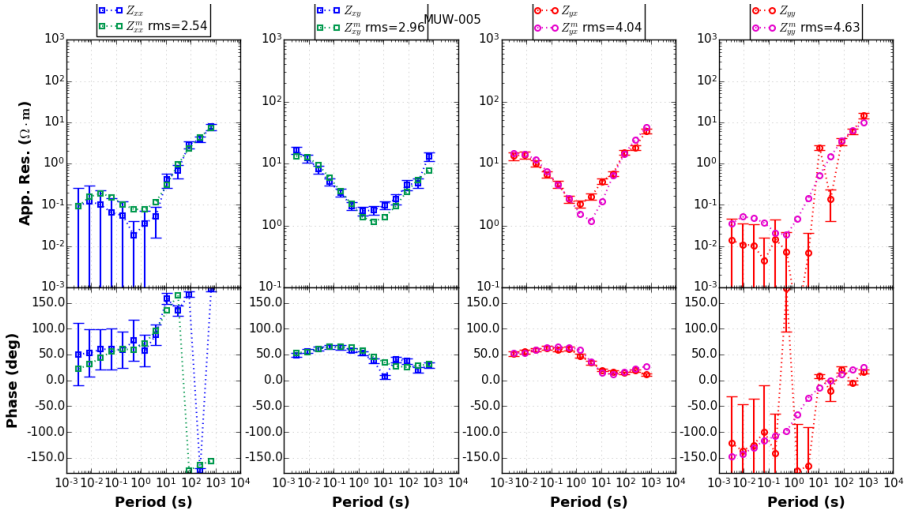

Figure 5: Model fitting curve for station MUW-005

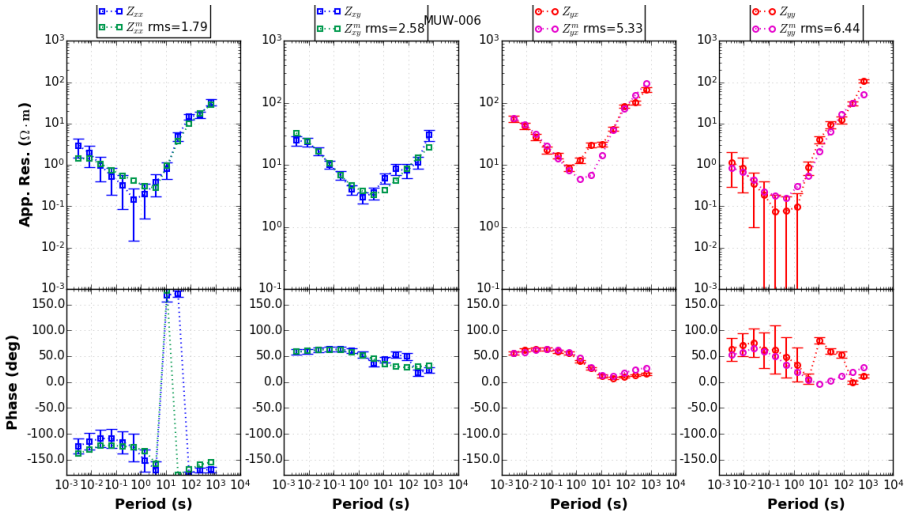

Figure 6: Model fitting curve for station MUW-006

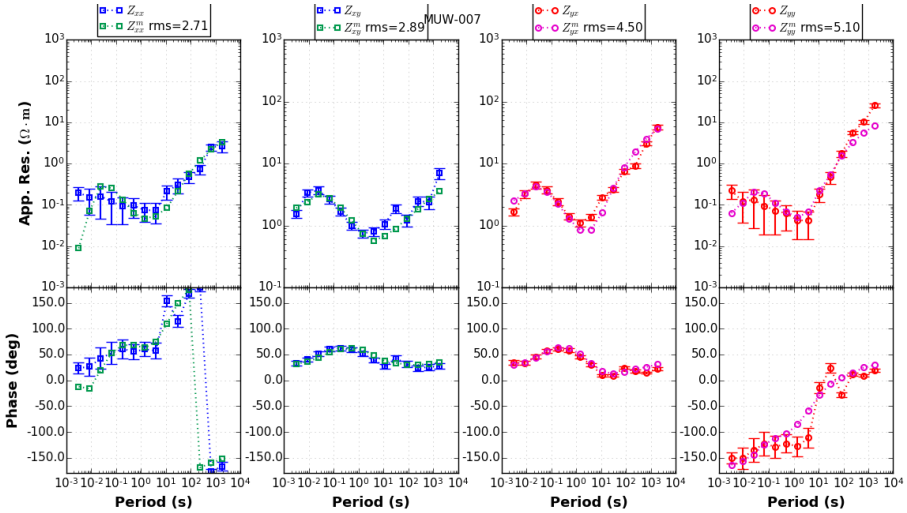

Figure 7: Model fitting curve for station MUW-007

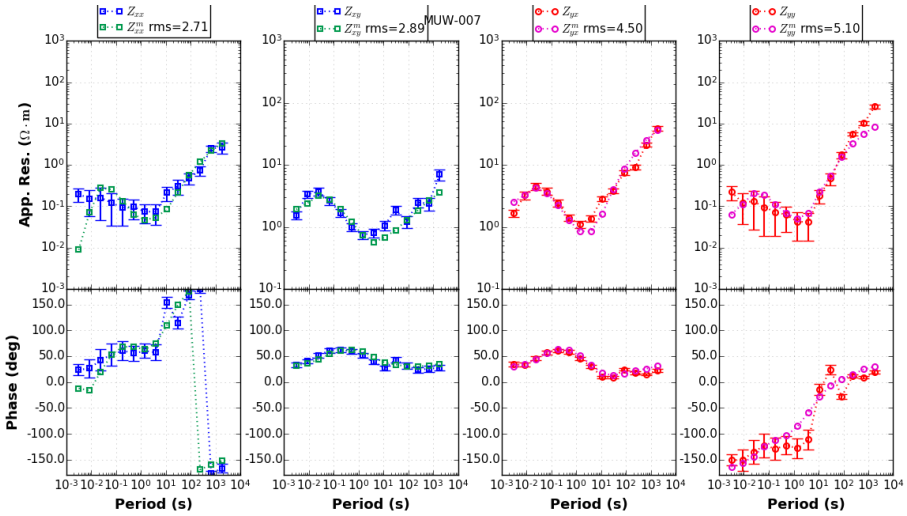

Figure 8: Model fitting curve for station MUW-007

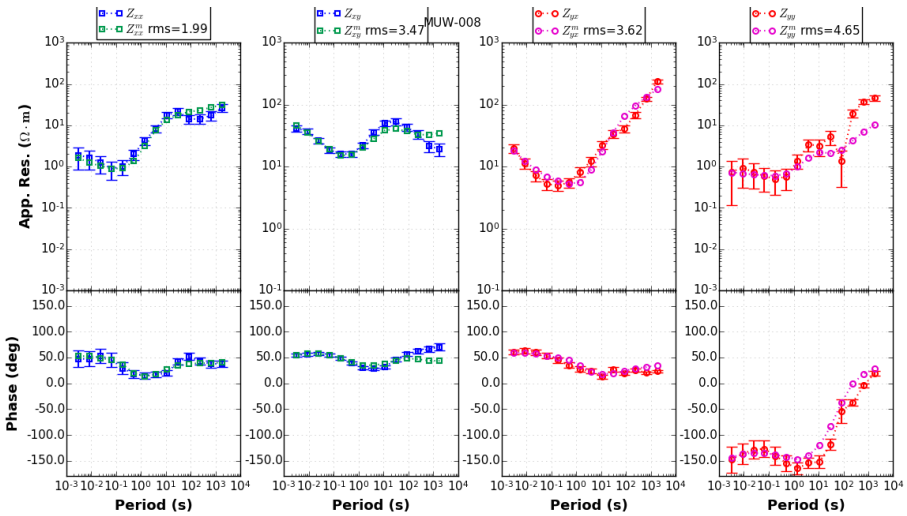

Figure 9: Model fitting curve for station MUW-008

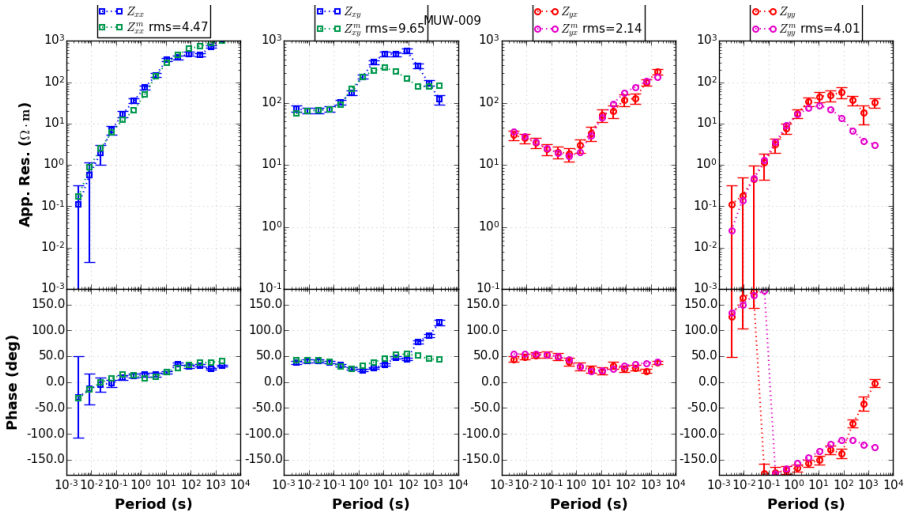

Figure 10: Model fitting curve for station MUW-009

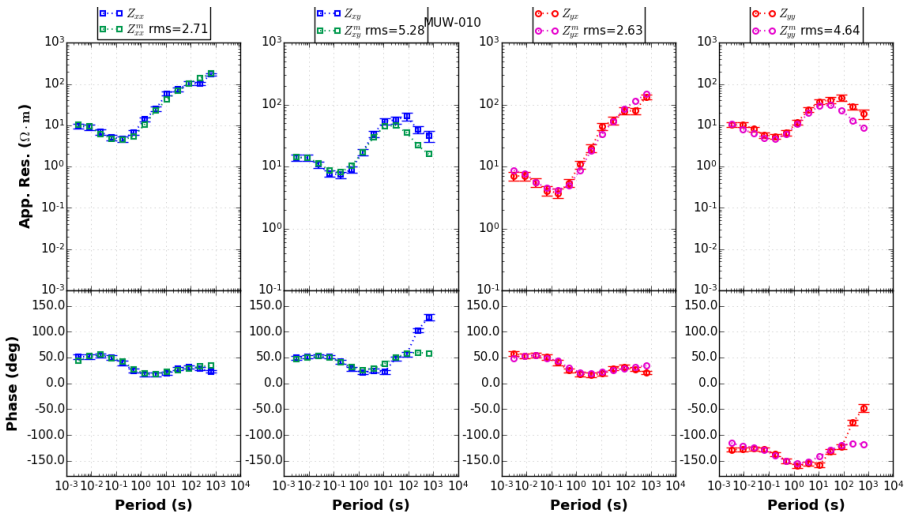

Figure 11: Model fitting curve for station MUW-010

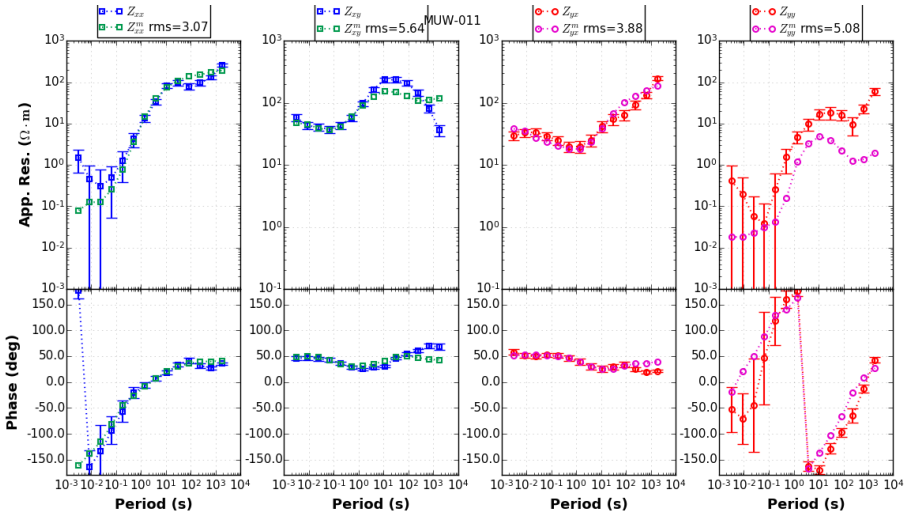

Figure 12: Model fitting curve for station MUW-011

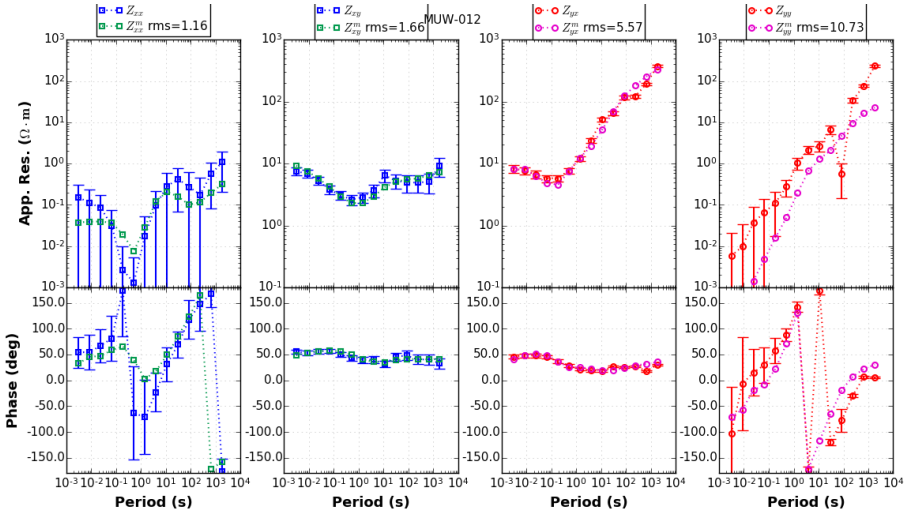

Figure 13: Model fitting curve for station MUW-012

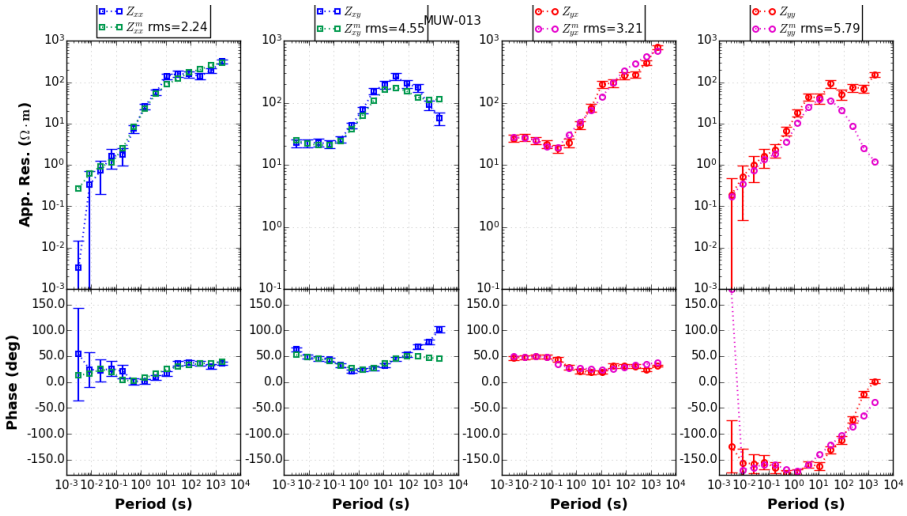

Figure 14: Model fitting curve for station MUW-013

Validity of the ModEM results - AMT fitting Curves

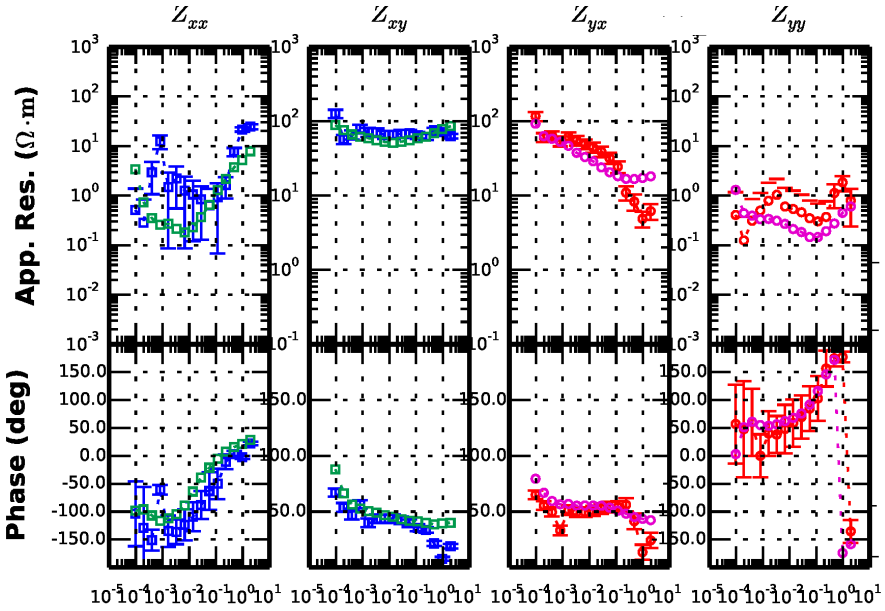

Figure 15: Model fitting curve for station mur001

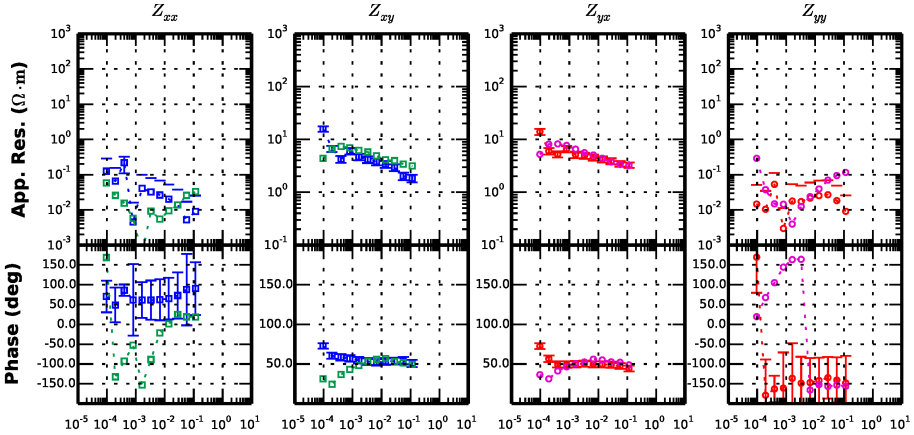

Figure 16: Model fitting curve for station mur002

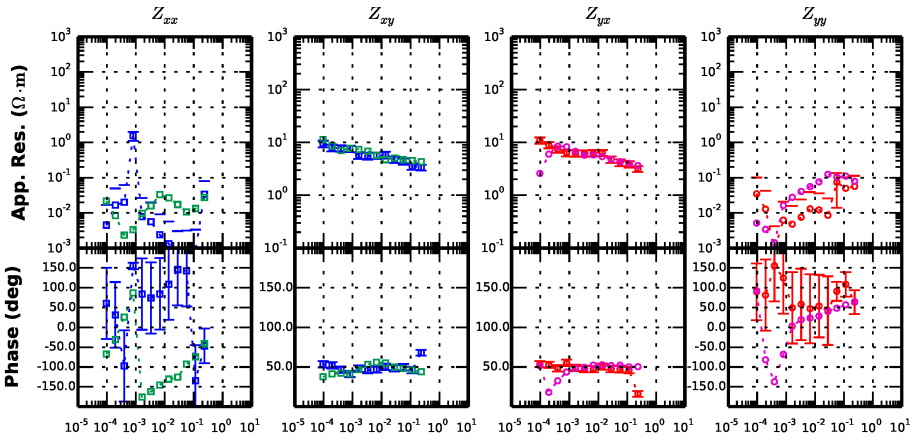

Figure 17: Model fitting curve for station mur003

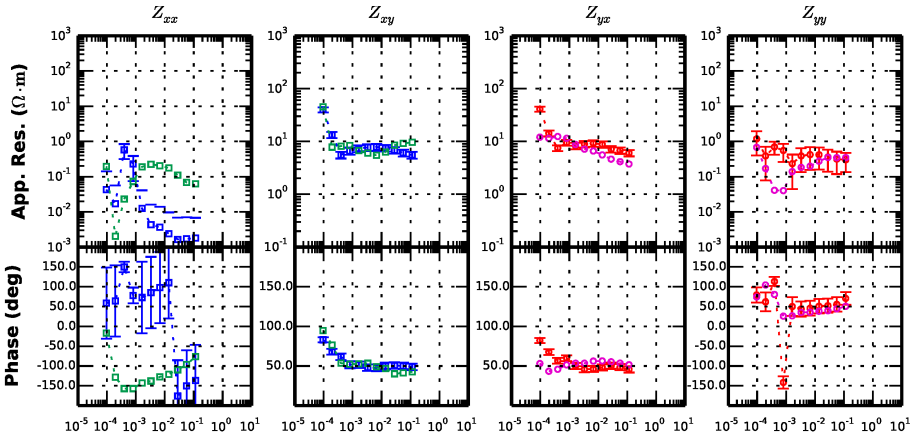

Figure 18: Model fitting curve for station mur004

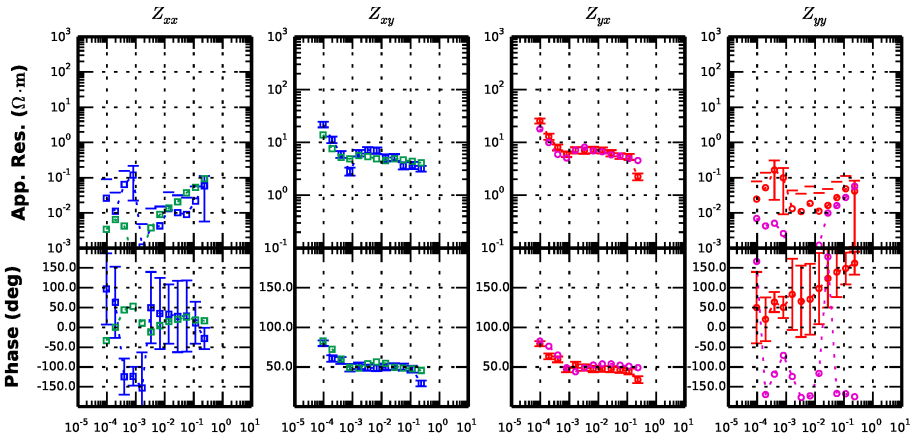

Figure 19: Model fitting curve for station mur005

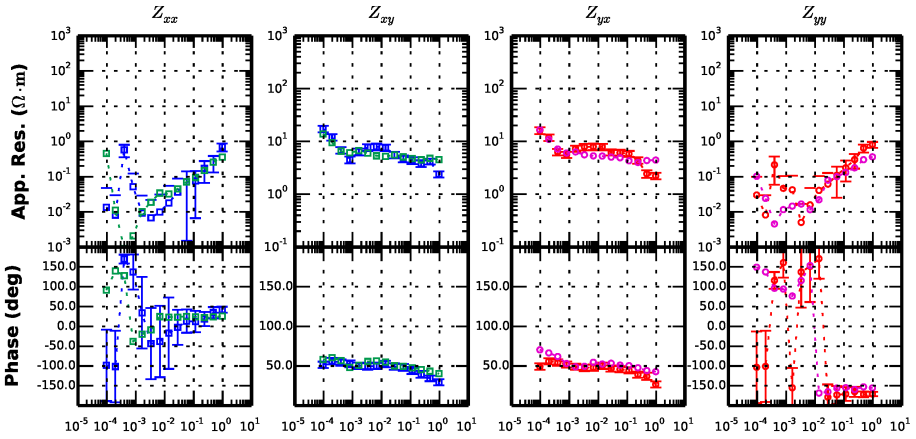

Figure 20: Model fitting curve for station mur006

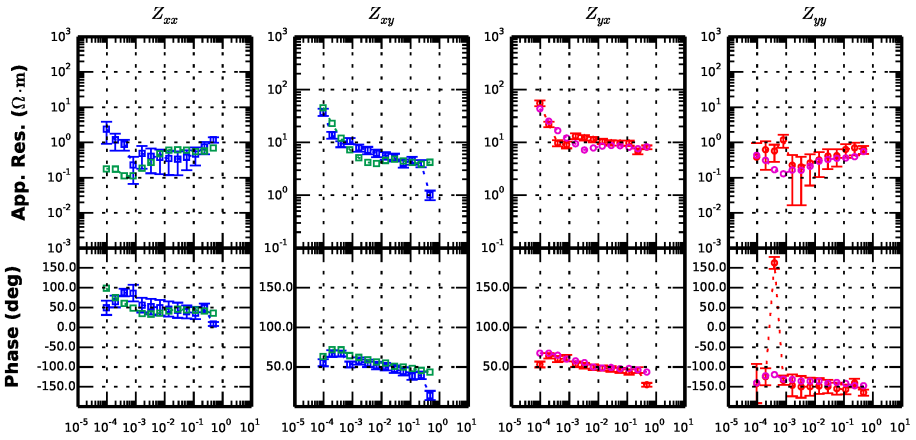

Figure 21: Model fitting curve for station mur007

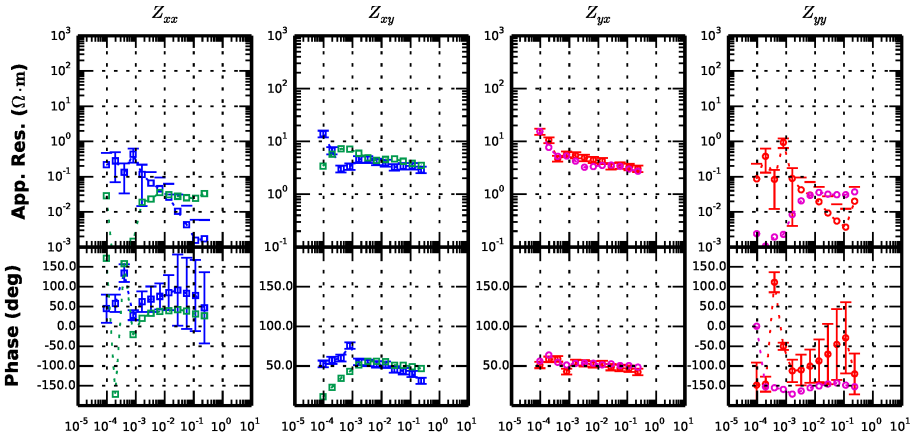

Figure 22: Model fitting curve for station mur008

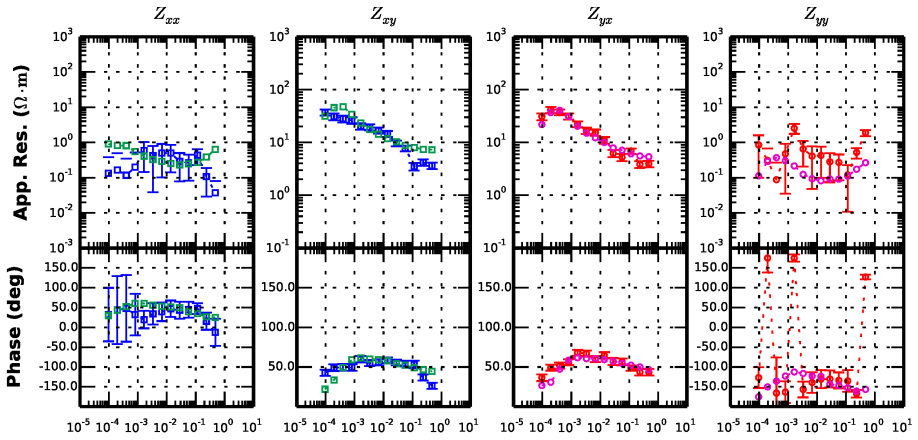

Figure 23: Model fitting curve for station mur009

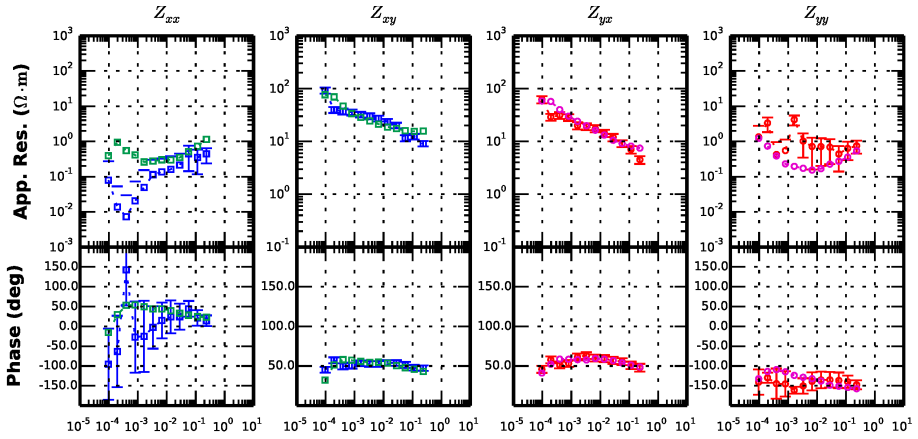

Figure 24: Model fitting curve for station mur010

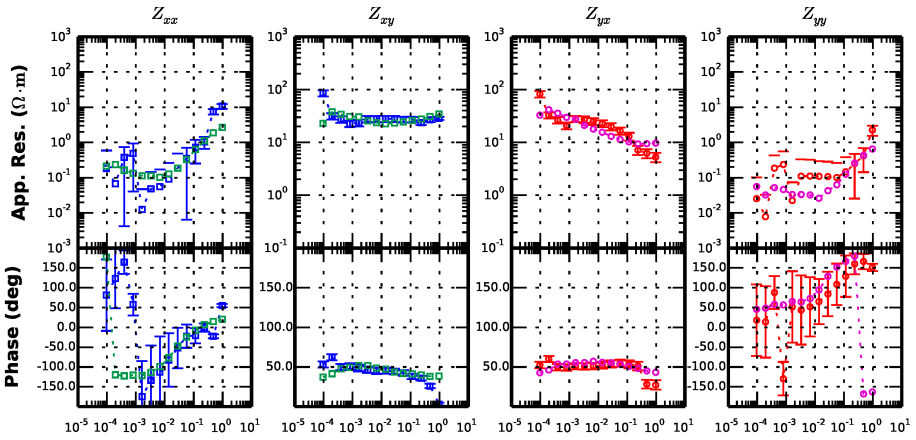

Figure 25: Model fitting curve for station mur011

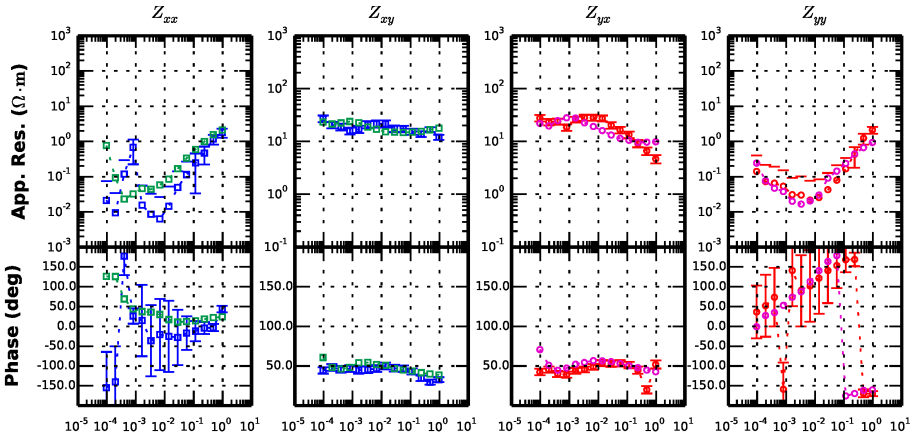

Figure 26: Model fitting curve for station mur012

WS3DINVMT Results

Searching for the smoothest model that fits the data, WSINV3DMT invokes an Occam approach (Constable et. al, 1988) based on data-space modeling to reduce computational disadvantages of model-space technique. Data-space approach reduces the number of parameters during the process of minimizing the penalty functional, so that the computational time and required memory are downsized explicitly. The code works on two different phases. Following the first phase that seeks for target RMS values, the algorithm starts to pursue a minimum-norm model in the second phase (Siripunvaraporn et al., 2005). For AMT data, the mesh was designed with evenly spaced 50m grid nodes near the center of study field, while mesh size was taken as 48 x 28 x 43 (including 7 air layers). A uniform initial model with homogeneous 100 Ωm electrical resistivity was used, where the thickness of the first layer is selected as 10 m. The cell sizes are designed with a vertical increment factor of 1.3 after the depth of 400 m was reached. In order to image the target area with higher resolution, cell sizes before 400 m was chosen manually to form a more densely structured grid. Total extents of the AMT model are 9 km, 7 km and 102.6 km for northing, easting and vertical directions respectively. The code ran with three periods per decade (17 in total) and error floors were chosen as 10.0 % and 5.0 %, respectively for the diagonal and off-diagonal elements. WSINV3DMT ran 5 iterations until target RMS of 1.95 was acquired (Figure 27).

Evaluation of wide-band MT data was in need of more complicated efforts due to larger data size and inherent coast effect. Initial model was designed as a half-space with 100 Ωm valued cells, while eastern and southern sides were fixed with 0.3 Ωm cells representing the Marmara Sea. Number of nodes was selected as 52 x 52 x 43. Thickness of the initial layer was chosen as 0.1 km, where the subsequent layers increase with a factor of 1.3. At the core of the mesh, horizontal extents of the cell sizes are chosen as 0.2 km. Run of the code ended up after 5th iteration by finalizing at a model with RMS of 4.7 (Figure 28, 29).

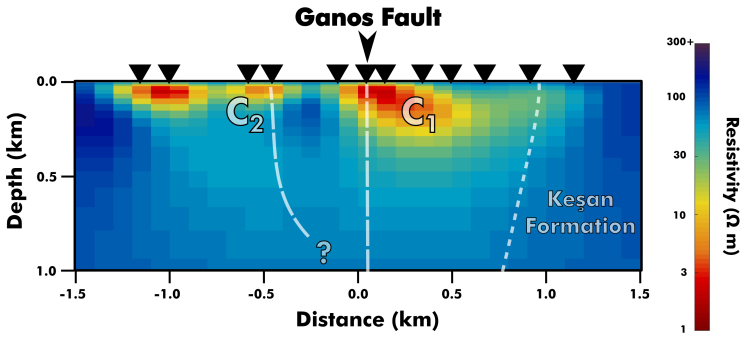

Figure 27: AMT results of WS3DINVMT modeling attempt.

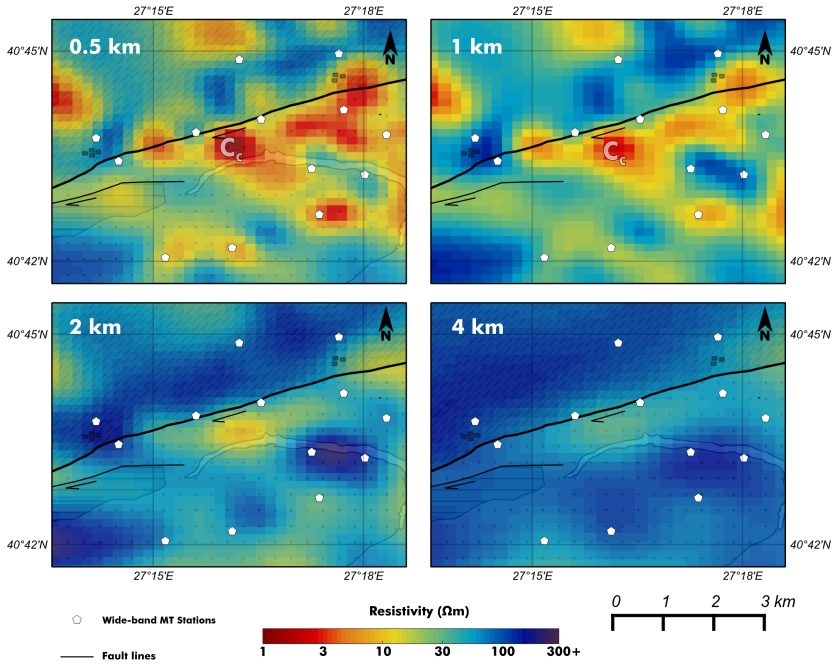

Figure 28: Depth slices of the resulting model of Wide-band MT data attained from WS3DINVMT.

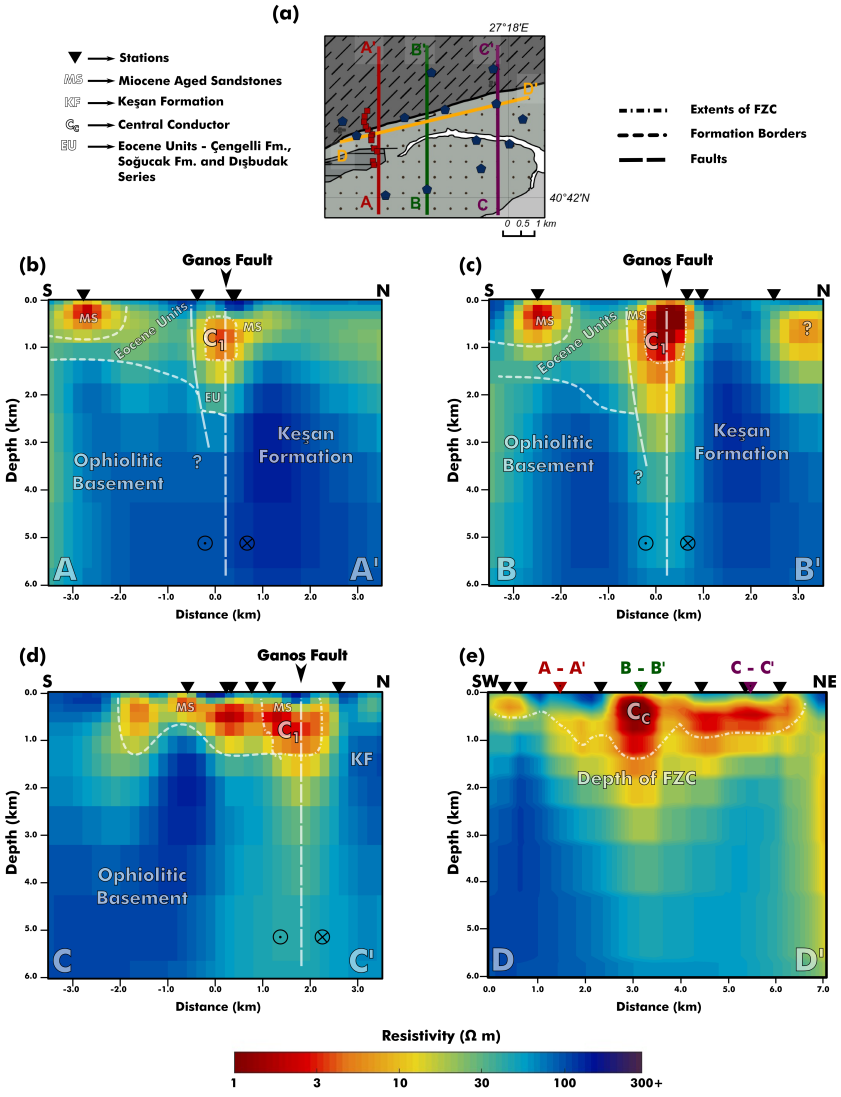

Figure 29: Cross sections of the resulting model of Wide-band MT data attained from WS3DINVMT.

2D AMT Model

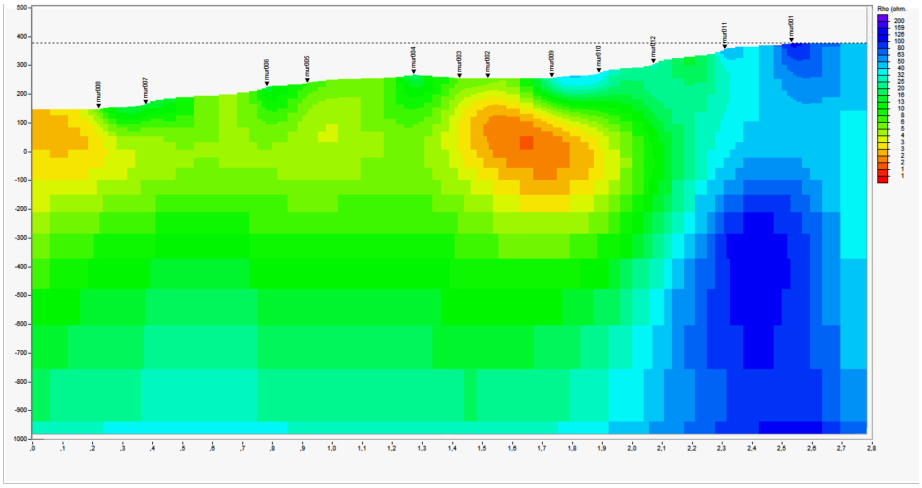

Figure 30: 2D AMT model attained by using WinGlink (Rodi and Mackie, 2001).

Skew Values

Skew values give information on dimensionality of individual MT measurements. As usually accepted among MT practitioners, skew-values above 0.3 considered as incompatible for one or two dimensional interpretation (Hoffmann-Rothe et al., 2004).

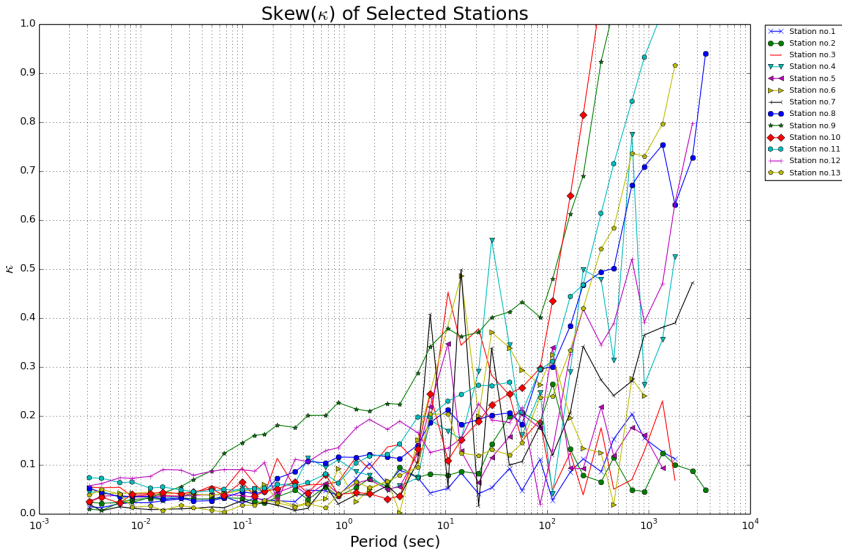

Figure 31: Skew values for wide-band MT stations

Figure 30 shows the skew values of wide-band MT stations. For values corresponding to $T > 10s$, three-dimensional structure starts to develop. Figure 31 demonstrates the skew values for AMT stations. Given the range of frequencies, most of the stations demonstrates low skew values, thus less three-dimensionality.

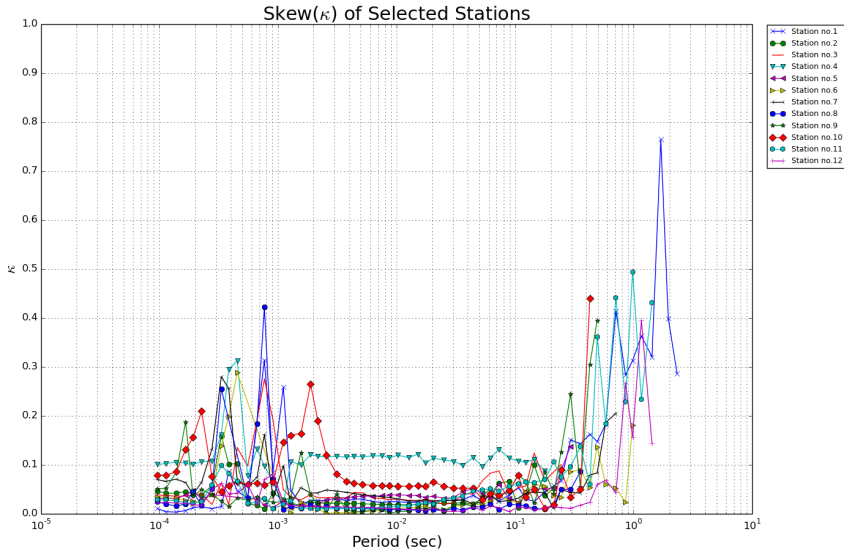

Figure 32: Skew values for AMT stations

References

Hoffmann−Rothe, A., Ritter, O., & Janssen, C. (2004). Correlation of electrical conductivity and structural damage at a major strike−slip fault in northern Chile. Journal of Geophysical Research: Solid Earth, 109(B10).

Rodi, W., & Mackie, R. L. (2001). Nonlinear conjugate gradients algorithm for 2-D magnetotelluric inversion. Geophysics, 66(1), 174-187.

Siripunvaraporn, W., Egbert, G., Lenbury, Y., Uyeshima, M. (2005) Three-dimensional magnetotelluric inversion: data-space method. Physics of the Earth and planetary interiors, 150(1), 3-14.